

# A star-forming galaxy at $z = 5.78$ in the *Chandra* Deep Field South

Andrew J. Bunker,<sup>1\*</sup> Elizabeth R. Stanway,<sup>1</sup> Richard S. Ellis,<sup>2</sup>  
Richard G. McMahon<sup>1</sup> and Patrick J. McCarthy<sup>3</sup>

<sup>1</sup>*Institute of Astronomy, University of Cambridge, Madingley Road, Cambridge CB3 0HA*

<sup>2</sup>*California Institute of Technology, Mail Stop 169-327, Pasadena, CA 91109, USA*

<sup>3</sup>*Carnegie Observatories, 813 Santa Barbara Street, Pasadena, CA 91101, USA*

Accepted 2003 March 25. Received 2003 March 24; in original form 2003 March 9

## ABSTRACT

We report the discovery of a luminous  $z = 5.78$  star-forming galaxy in the *Chandra* Deep Field South. This galaxy was selected as an ‘*i*-drop’ from the GOODS public survey imaging with the *Hubble Space Telescope*/Advanced Camera for Surveys (object 3 in the work of Stanway, Bunker & McMahon 2003). The large colour of  $(i' - z')_{\text{AB}} = 1.6$  indicated a spectral break consistent with the Lyman  $\alpha$  forest absorption shortward of Lyman  $\alpha$  at  $z \approx 6$ . The galaxy is very compact (marginally resolved with ACS with a half-light radius of 0.08 arcsec, so  $r_{\text{hl}} < 0.5 h_{70}^{-1}$  kpc). We have obtained a deep (5.5 h) spectrum of this  $z'_{\text{AB}} = 24.7$  galaxy with the DEIMOS optical spectrograph on the Keck Telescope, and here we report the discovery of a single emission line centred on 8245 Å detected at  $20\sigma$  with a flux of  $f \approx 2 \times 10^{-17}$  erg  $\text{cm}^{-2}$   $\text{s}^{-1}$ . The line is clearly resolved with detectable structure at our resolution of better than 55  $\text{km s}^{-1}$ , and the only plausible interpretation consistent with the ACS photometry is that we are seeing Lyman  $\alpha$  emission from a  $z = 5.78$  galaxy. This is the highest redshift galaxy to be discovered and studied using *HST* data. The velocity width ( $\Delta v_{\text{FWHM}} = 260$   $\text{km s}^{-1}$ ) and rest-frame equivalent width ( $W_{\text{rest}}^{\text{Ly}\alpha} = 20$  Å) indicate that this line is most probably powered by star formation, as an AGN would typically have larger values. The starburst interpretation is supported by our non-detection of the high-ionization N V  $\lambda 1240$ -Å emission line, and the absence of this source from the deep *Chandra* X-ray images. The star formation rate inferred from the rest-frame UV continuum is  $34 h_{70}^{-2} M_{\odot} \text{yr}^{-1}$  ( $\Omega_{\text{M}} = 0.3$ ,  $\Omega_{\Lambda} = 0.7$ ). This is the most luminous starburst known at  $z > 5$ . Our spectroscopic redshift for this object confirms the validity of the *i*'-drop technique of Stanway et al. to select star-forming galaxies at  $z \approx 6$ .

**Key words:** galaxies: evolution – galaxies: formation – galaxies: high-redshift – galaxies: individual: SBM03#3 – galaxies: starburst – ultraviolet: galaxies.

## 1 INTRODUCTION

A key question in modern cosmology is the star formation rate of galaxies in the young Universe. In the past few years, the Lyman break technique (Steidel, Pettini & Hamilton 1995) has proved very successful in identifying star-forming galaxies at  $z = 3$ –4, through their rest-frame ultraviolet continuum absorbed by the Lyman  $\alpha$  forest of the intergalactic medium at  $\lambda_{\text{rest}} < 1216$  Å (e.g. Steidel et al. 1996, 1999). In a recent paper (Stanway et al. 2003) we have pushed this technique to even earlier epochs, using the latest public data from the Great Observatories Origins Deep Survey (GOODS: Dickinson & Giavalisco 2002), taken with the new Advanced Camera for Surveys (ACS: Ford et al. 2002) on the *Hubble Space Telescope* (*HST*). By selecting on extreme colours between the F775W

*i*' and F850LP *z*' filters, we identify galaxies in the *Chandra* Deep Field South (CDF-S) with  $(i' - z')_{\text{AB}} > 1.5$  that are likely to be at redshifts  $5.6 < z < 6.5$ . In this Letter we report on our spectroscopic confirmation with Keck/DEIMOS of one of our candidates – object 3 in Stanway et al. (2003), hereafter called SBM03#3 (Fig. 3, later). We show that this  $z'_{\text{AB}} = 24.7$  galaxy has Lyman  $\alpha$  emission at a redshift of  $z = 5.78$ , and does indeed lie within the expected redshift range. This confirms the validity of the *i*'-drop technique of Stanway et al. (2003).

## 2 OBSERVATIONS AND DATA REDUCTION

We observed SBM03#3 ( $\alpha_{2000} = 03^{\text{h}}32^{\text{m}}25^{\text{s}}.59$ ,  $\delta_{2000} = -27^{\circ}55'48''.4$ : Stanway et al. 2003) on the nights of UT 2003 January 8 and 9, using the new Deep Imaging Multi-Object Spectrograph (DEIMOS: Davis et al. 2002; Phillips et al. 2002) at the Cassegrain

\*E-mail: bunker@ast.cam.ac.uk

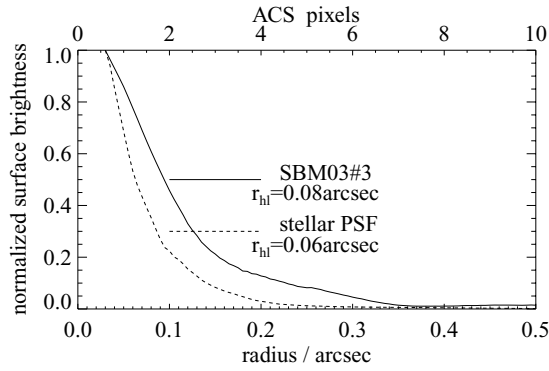


**Figure 1.** The normalized radial surface brightness profile of SBM03#3 from the *HST*/ACS F850LP  $z'$ -band image, compared with that of a star. The high- $z$  galaxy is only marginally resolved.

focus of the 10-m Keck II Telescope. DEIMOS has eight MIT/LL  $2k \times 4k$  CCDs with  $15\text{-}\mu\text{m}$  pixels and an angular pixel scale of  $0.1185 \text{ arcsec pixel}^{-1}$ . We used a slitmask to target various objects in the CDF-S over the  $16.5 \times 5 \text{ arcmin}^2$  DEIMOS field, as part of an ongoing programme to obtain spectra of objects with extreme optical/near-infrared colours (to be reported elsewhere). Each slitlet was 1 arcsec wide, and the slit containing SBM03#3 was at the extreme edge of the field, so, although the slit was 100 arcsec long, the target was only 3 arcsec from the slit edge. The observations were obtained using the Gold 1200 line  $\text{mm}^{-1}$  grating in first order blazed at  $\lambda_{\text{blaze}} = 7500 \text{ \AA}$ , producing a dispersion of  $0.320 \text{ \AA pixel}^{-1}$ . The grating was tilted to sample the wavelength range  $\lambda_{\text{obs}} 7100\text{--}9700 \text{ \AA}$ , corresponding to a rest-frame wavelength of  $\lambda_{\text{rest}} 1047\text{--}1430 \text{ \AA}$  at the redshift of SBM03#3 ( $z = 5.78$ , see Section 3.1). A small region in the middle of the wavelength range  $\lambda_{\text{obs}} 8405\text{--}8412 \text{ \AA}$  is unobserved as it falls in the gap between two CCDs. We used the OG550 order-blocking filter to remove all light at wavelengths shortward of  $5500 \text{ \AA}$ , so we should not be affected by second-order light.

The spectral resolution was measured to be  $\Delta\lambda_{\text{FWHM}}^{\text{obs}} \approx 1.35\text{--}1.50 \text{ \AA}$  from the sky lines and those of reference arc lamps ( $\Delta v_{\text{FWHM}} = 55 \text{ km s}^{-1}$ , a resolving power of  $\lambda/\Delta\lambda_{\text{FWHM}} = 5500$ ). As the seeing disc (typically  $0.7 \text{ arcsec FWHM}$ ) was smaller than the slit width of  $1.0 \text{ arcsec}$ , the true resolution is somewhat better for a source that does not fill the slit.

The observations spanned an airmass range of 1.4–1.6. The position angle (PA) of slits on the mask was  $6^\circ$ , chosen to be close north–south ( $0^\circ$ , the parallactic angle) as the field was observed

during meridian transit. A total of 20 ks of on-source integration was obtained, and this was broken into individual exposures each of duration 2400 s to enable more effective cosmic ray rejection. We dithered the telescope  $1.5 \text{ arcsec}$  along the slit between integrations. The spectrophotometric standard star HZ 44 (Massey et al. 1988; Massey & Gronwall 1990) was observed to determine the sensitivity function. The flux calibration was checked with the spectra of the five alignment stars of known broad-band photometry ( $I \approx 17\text{--}19 \text{ mag}$ ), used to position the CDF-S mask through  $2 \times 2 \text{ arcsec}^2$  alignment boxes.

The data reduction followed standard procedures using IRAF. Each frame first had the bias subtracted, determined from the overscan region appropriate to that CCD. Contemporaneous flat-fields were obtained with a halogen lamp immediately after the science exposures, and these internal flats were normalized through division by the extracted lamp spectrum, and corrected for non-uniform illumination of the slit by comparison with twilight sky and dome spectral flat-fields. Wavelength calibration was obtained from Ne+Ar+Hg+Kr reference arc lamps, and a cubic fit to the centroids of  $\approx 20$  arc lines for each CCD created a wavelength solution with rms residuals of  $0.02 \text{ \AA}$ . The wavelength calibration was checked with the centroids of prominent sky lines. The spectrum was then rectified (straightening the sky lines), and sky subtraction was performed by a fifth-order polynomial fit to each rectified detector column (parallel to the slit), excluding from the fit those regions occupied by sources.

### 3 RESULTS

#### 3.1 The redshift of SBM03#3

The combined 5.5 h of DEIMOS spectroscopy showed a clear emission line detected at  $20\sigma$  at the location in the slit corresponding to the expected position of galaxy SBM03#3. The peak of the line emission is at  $\lambda_{\text{obs}} = 8245.4 \pm 0.9 \text{ \AA}$ , and the integrated flux is within 30 per cent of  $f = 2 \times 10^{-17} \text{ erg cm}^{-2} \text{ s}^{-1}$ , extracting over 17 pixels (2 arcsec) and measuring between the zero-power points (8242–8260  $\text{\AA}$ ). This is actually a lower limit on the line flux because of possible slit losses if the emission line is spatially extended, although this is probably negligible since the galaxy is very compact (Fig. 1). The flux measurement is consistent over both nights. The emission line is not seriously contaminated by residuals from strong OH lines but does straddle a weak complex of sky lines. Fig. 2 shows the combined two-dimensional long-slit spectrum around this emission line.

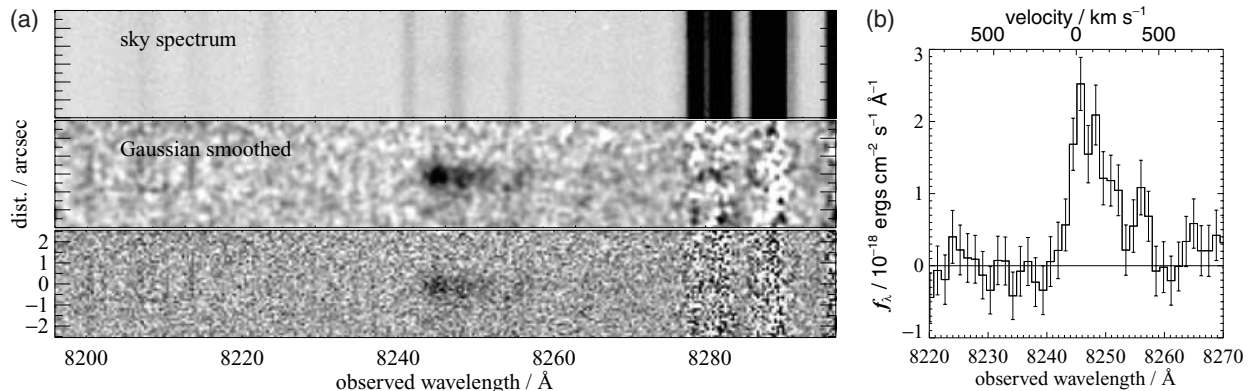


**Figure 2.** (a) The lower panel shows the 2D spectrum around Lyman  $\alpha$  ( $100 \text{ \AA}$  by 5 arcsec), the middle panel shows this smoothed with a Gaussian of  $\sigma = 1$  pixel, and the upper panel shows the sky spectrum for this wavelength range. (b) The one-dimensional spectrum around Lyman  $\alpha$ , extracted over a 9-pixel ( $1 \text{ arcsec}$ ) width. The data have been binned into independent resolution elements of  $1.3 \text{ \AA}$  (4 pixels).

Single-line redshifts are often open to question, but the most probable identification of this solo emission line is Lyman  $\alpha$   $\lambda 1215.8 \text{ \AA}$  at  $z = 5.7825 \pm 0.001$ , given that this galaxy was pre-selected as an  $i'$ -drop to have a photometric redshift of  $z \approx 6$ . We briefly consider (and rule out) other possible redshift assignments. This line emission is extremely unlikely to be H $\beta$   $\lambda 4861.3 \text{ \AA}$  or [O III]  $\lambda\lambda 5006.8, 4958.9 \text{ \AA}$  at  $z \approx 0.7$  as we do not detect the other nearby lines in this complex. If this line emission were [O II]  $\lambda\lambda 3726.1, 3728.9 \text{ \AA}$  at  $z = 1.212$ , we would expect to resolve comfortably the [O II] doublet with our spectral resolution of  $55 \text{ km s}^{-1}$ , as demonstrated by Davis et al. (2002) using DEIMOS in the same configuration. The most probable interpretation is that we are seeing Lyman  $\alpha$   $\lambda 1215.8 \text{ \AA}$  at  $z = 5.78$ . The only plausible alternative to high-redshift Lyman  $\alpha$  is H $\alpha$   $\lambda 6562.8 \text{ \AA}$  at  $z = 0.256$ : however, the H $\alpha$  interpretation would not produce the large flux decrement observed between the  $z'$  band and  $i'$  band. Hence we conclude that Lyman  $\alpha$  emission at  $z = 5.78$ , associated with the  $i'$ -drop galaxy SBM03#3, is by far the most probable identification of the line [see Stern et al. (2000) for a discussion of one-line redshift determinations for high- $z$  galaxies].

### 3.2 Spectral profile of the Lyman $\alpha$ emission

The Lyman  $\alpha$  line is clearly resolved spectrally at this  $55 \text{ km s}^{-1}$  resolution, with significant velocity structure evident (Fig. 2). There appears to be a weak second peak of emission slightly to the red of the main Lyman  $\alpha$  emission, around  $8256 \text{ \AA}$ , and there is more marginal evidence for narrow absorption at the core of the main emission line.

The spectral width of the Lyman  $\alpha$  line is  $7.3 \pm 0.5$  pixel FWHM, excluding the second peak at  $8256 \text{ \AA}$ . This is equivalent to a velocity width of  $\Delta v_{\text{FWHM}} = 260 \pm 20 \text{ km s}^{-1}$  after deconvolution with the instrumental width. The linewidth is similar to those of other  $z \approx 6$  galaxies (e.g. Rhoads et al. 2003; Kodaira et al. 2003; Lehnert & Bremer 2003). The Lyman  $\alpha$  profile is asymmetric, with a pronounced red wing but a sharper decline in flux density on the blue side (Fig. 2). This appears to be a common feature in high- $z$  starbursts with Lyman  $\alpha$  in emission (e.g. Lowenthal et al. 1997; Dey et al. 1998; Bunker, Moustakas & Davis 2000; Ellis et al. 2001), and is most likely due to an outflow of neutral hydrogen, where we only see the back-scattered Lyman  $\alpha$  from the far side of the expanding nebula – only the photons on the red side of the resonant Lyman  $\alpha$  emission-line profile can escape, with the blue wing being absorbed by neutral gas (within the galaxy and in the Lyman  $\alpha$  forest). The P Cygni-like profile of Lyman  $\alpha$  is consistent with this outflow model. Hence the profile of Lyman  $\alpha$  is skewed to the red, so the systemic redshift determined from the peak of the emission may be overestimated. Near-infrared spectroscopy by Pettini et al. (2001) of the rest-frame optical forbidden lines and Balmer lines in  $z \approx 3$  galaxies shows a  $200\text{--}1100 \text{ km s}^{-1}$  redshifting of the Lyman  $\alpha$  relative to the nebular emission lines.

The velocity dispersion of  $\sigma_{\text{LOS}} = 110 \pm 10 \text{ km s}^{-1}$  inferred from the linewidth of Lyman  $\alpha$  is likely to be a lower limit, as the line profile is truncated. However, the velocity width of Lyman  $\alpha$  cannot be reliably used to estimate the galaxy mass as it is unlikely to be representative of the true velocity dispersion, since resonant scattering will broaden the spectral profile of the escaping photons (e.g. Binette et al. 1993).

### 3.3 AGN or starburst?

Careful inspection of the spectrum did not reveal any lines at other wavelengths in the same spatial location as the Lyman  $\alpha$  emission.

The only other significant line that should fall within our spectral coverage (although close to the gap between the CCDs) is the high-ionization rest-ultraviolet doublet N v  $\lambda\lambda 1238.8, 1242.8 \text{ \AA}$ , which is usually prominent in active galactic nuclei (AGN). Our flux limits at  $8402$  and  $8429 \text{ \AA}$  are  $f < 2 \times 10^{-18} \text{ erg cm}^{-2} \text{ s}^{-1}$  ( $3\sigma$ ), conservatively assuming the lines are extended and that half the light is lost in gap between the CCDs at  $8405\text{--}8412 \text{ \AA}$ . Our lower limit of  $f(\text{Ly}\alpha)/f(\text{N v}) > 10$  ( $3\sigma$ ) compares with the typical line ratios from composite QSO spectra of  $f(\text{Ly}\alpha)/f(\text{N v}) = 4.0$  (Osterbrock 1989). Hence the non-detection of N v  $1240 \text{ \AA}$  favours the interpretation that the Lyman  $\alpha$  arises from the Lyman continuum flux produced by OB stars, rather than the harder ultraviolet spectrum of a QSO. The velocity width of Lyman  $\alpha$  ( $260 \text{ km s}^{-1}$  FWHM) is also significantly smaller than seen in the broad-line regions of AGN, even after correcting for the self-absorbed blue wing (Section 3.2), again suggesting a starburst rather than an AGN. SBM03#3 is undetected in the *Chandra* X-ray map of the CDF-S (Giacconi et al. 2002) to  $2\sigma$  limits of  $5.5 \times 10^{-17}$  and  $4.5 \times 10^{-16} \text{ erg cm}^{-2} \text{ s}^{-1}$  in the soft ( $0.5\text{--}2 \text{ keV}$ ) and hard ( $2\text{--}10 \text{ keV}$ ) X-ray bands respectively. We note that several other Lyman  $\alpha$  emitters at high redshift are also undetected in X-rays (Malhotra et al. 2003).

### 3.4 Continuum shape and Lyman $\alpha$ equivalent width

We do not have a significant detection of the the continuum in the Keck/DEIMOS spectroscopy, but the flux measurement of  $z'_{\text{AB}} = 24.67 \pm 0.03$  from the *HST*/ACS F850LP  $z'$ -band image – which encompasses the redshifted Lyman  $\alpha$  line at its blue end – enables us to determine the equivalent width of this line and the continuum flux density ( $L_{\nu} = 2.7 h_{70}^{-1} \times 10^{29} \text{ erg s}^{-1} \text{ Hz}^{-1}$  at  $\lambda_{\text{rest}} \approx 1300 \text{ \AA}$ , where we assume  $\Omega_{\text{M}} = 0.3$  and  $\Omega_{\Lambda} = 0.7$  throughout). The emission line has a luminosity  $L = (7 \pm 2) \times 10^{42} h_{70}^{-1} \text{ erg s}^{-1}$  and accounts for only  $\approx 4$  per cent of the  $z'$ -band flux and  $\sim 25$  per cent of the  $i'$ -band flux, and, once the effect of this line contamination of the broad-band magnitudes is removed, the equivalent width of the line is  $W_{\text{obs}}^{\text{Ly}\alpha} = 140 \pm 50 \text{ \AA}$  in the observed frame, assuming that there is negligible continuum flux below  $8245 \text{ \AA}$  (shortward of  $\lambda_{\text{rest}} 1216 \text{ \AA}$ , the Lyman  $\alpha$  line) due to absorption by the Lyman  $\alpha$  forest.

The rest-frame equivalent width at  $z = 5.78$  is  $W_{\text{rest}}^{\text{Ly}\alpha} = 20 \pm 7 \text{ \AA}$  which is within the realm of what is observed in star-forming galaxies. From stellar synthesis models of star-forming regions (e.g. Charlot & Fall 1993), the theoretical Lyman  $\alpha$  equivalent width for a young region of active star formation is  $W_{\text{rest}}^{\text{Ly}\alpha} \approx 100\text{--}200 \text{ \AA}$ . However, the observed Lyman  $\alpha$  emission from star-forming galaxies is invariably much weaker, typically  $W_{\text{rest}} = 5\text{--}30 \text{ \AA}$  (e.g. Steidel et al. 1996; Warren & Møller 1996), or even in absorption. The rest-frame equivalent width for SBM03#3 lies at the upper end of this observed range and is similar to the narrow-band selected galaxies at  $z > 5.5$  (Hu, McMahon & Cowie 1999; Hu et al. 2002; Kodaira et al. 2003).

From the  $z'$  band, the ultraviolet continuum implies an unobscured star formation rate of  $33.8 h_{70}^{-1} M_{\odot} \text{ yr}^{-1}$  (Stanway et al. 2003). The star formation rate inferred from the Lyman  $\alpha$  emission would be  $\approx 5$  times less than this, probably due to selective extinction of this line through resonant scattering. SBM03#3 has the highest ultraviolet luminosity (i.e. the largest unobscured star formation rate) of any starburst yet found at  $z > 5.5$ .

We obtained 10 ks of near-infrared imaging with a  $K_s$  filter ( $\lambda_{\text{cent}} = 2.15 \text{ \mu m}$ , equivalent to  $\lambda_{\text{rest}} = 3200 \text{ \AA}$ ) using the Wide Field Infrared Camera (WIRC) camera on the Las Campanas 2.5-m du Pont telescope on the night of 2003 February 20 UT (Fig. 3, opposite p. L51). The seeing was  $0.7$  arcsec, oversampled by the

0.1-arcsec pixels of the 1024<sup>2</sup> Rockwell HgCdTe array. The galaxy SBM03#3 was undetected, with a  $2\sigma$  limiting magnitude of  $K_s > 20.6$  (Vega magnitudes). If the spectrum longward of Lyman  $\alpha$  is a power law, we can constrain the slope to be  $\alpha < 0.4$  (where  $f_\lambda \propto \lambda^\alpha$ ) from  $(z'_{AB} - K_s) < 4.1 (2\sigma)$ .

Knowing the redshift and the contamination of the broad-band magnitudes by the line emission, the continuum depression as inferred from the  $(i' - z')_{AB} = 1.60 \pm 0.13$  colour may be used to make a direct estimate of  $D_A$ , the absorption due to intervening cosmological H I clouds at  $z \approx 4.8\text{--}5.8$ . Outflowing neutral hydrogen intrinsic to the source may also play a significant role in absorbing the blue-wing of Lyman  $\alpha$ . Formally, the  $D_A$  continuum break (Oke & Korycansky 1982) is defined as

$$D_A = \left[ 1 - \frac{f_v(1050\text{--}1170 \text{ \AA})_{\text{obs}}}{f_v(1050\text{--}1170 \text{ \AA})_{\text{pred}}} \right] \quad (1)$$

(e.g., Schneider, Schmidt, & Gunn 1991; Madau 1995). The *HST*/ACS F775W  $i'$  band samples the rest-frame at 1030–1220 Å, and the measured magnitude is  $i'_{AB} = 26.27 \pm 0.13$  (Stanway et al. 2003). After correcting for the fraction of the  $i'$  and  $z'$  filters that lie above the redshifted 1216-Å break, we calculate  $D_A = 0.95^{+0.05}_{-0.10}$  assuming an intrinsic spectral shape of  $f_\lambda \propto \lambda^{-1.1}$ , the average for the  $z \approx 3$  Lyman break galaxies (Meurer et al. 1997). This is consistent with the values derived from Sloan Digital Sky Survey quasars at similar redshifts by Fan et al. (2001).

### 3.5 The size of SBM03#3

The galaxy SBM03#3 is very compact in the *HST* images (Fig. 1) – in the highest signal-to-noise ratio ACS  $z'$  image it is only marginally resolved with a half-light radius of  $r_{\text{hl}} = 0.08$  arcsec (Stanway et al. 2003), compared with  $r_{\text{hl}} = 0.06$  arcsec for unsaturated stars in the ACS image. Hence the half-light radius of the star-forming region at  $z = 5.78$  must be  $r_{\text{hl}} \ll 0.5 h_{70}^{-1}$  kpc. This is very compact, and corresponds to the physical size of dwarf spheroidals at lower redshift. SBM03#3 is more compact than typical Lyman-break galaxies at  $z \approx 3$ : Lowenthal et al. (1997) find a median  $r_{\text{hl}} = 3.5 h_{70}^{-1}$  kpc and a range  $1.7 < r_{\text{hl}} < 7 h_{70}^{-1}$  kpc. We have also compared the spatial extent of the line emission with a cross-cut of an alignment star in the same slit-mask (i.e. identical seeing and airmass): the Lyman  $\alpha$  line has a very compact spatial extent, unresolved in  $\approx 0.7$  arcsec FWHM seeing, so this seems not to be one of the cases where the Lyman  $\alpha$  emission-line morphology is significantly more extended than the continuum (e.g. Steidel et al. 2000; Bunker et al. 2000).

## 4 CONCLUSIONS

We have obtained deep spectroscopy with Keck/DEIMOS of SBM03#3, an  $i'$ -drop in the *Chandra* Deep Field South photometrically selected from *HST*/ACS images to lie at  $z \approx 6$ . We discover a single emission line with peak intensity at 8245 Å, consistent with Lyman  $\alpha$  emission from a galaxy at  $z = 5.78$ . The spectrally resolved profile of the emission line is asymmetric (as high- $z$  Lyman  $\alpha$  tends to be) with a P Cygni-like profile and a sharp cut-off on the blue wing. The line flux is  $\approx 2 \times 10^{-17}$  erg cm<sup>-2</sup> s<sup>-1</sup>. The equivalent width inferred from the  $z'$ -band photometry from *HST*/ACS is  $W_{\text{rest}} = 20$  Å, which is within the range seen in high- $z$  star-forming galaxies. The galaxy is undetected in X-rays by *Chandra* and the velocity width of the Lyman  $\alpha$  is comparatively small ( $v_{\text{FWHM}} = 260$  km s<sup>-1</sup>), and we do not detect the high-ionization line N V  $\lambda 1240$  Å, all of which support the view that this line emission is powered by star formation rather than an AGN. Our spectroscopic

redshift for this object confirms the validity of the  $i'$ -drop selection technique of Stanway et al. (2003) to select star-forming galaxies at  $z \approx 6$ .

The relatively bright rest-frame ultraviolet continuum flux and Lyman  $\alpha$  line luminosity of SBM03#3 and the recent *WMAP* results which indicate the epoch of reionization to lie at  $z > 10$  (Kogut et al. 2003) bode well for searches for ultraviolet-luminous star-forming galaxies at  $z > 7$ , such as those that will be possible using the narrow-band near-infrared imaging system DAZLE (the Dark Ages ‘Z’ Lyman Explorer: McMahon et al., in preparation), *HST*/WFC3 and James Webb Space Telescope.

## ACKNOWLEDGMENTS

We are extremely grateful for the help and support that we received while observing at Keck, and in particular thank Greg Wirth, Bob Goodrich and Chuck Sorenson. We used Drew Phillips’ extremely useful DSIMULATOR software for slit-mask design. We have had useful discussions on the reduction of optical slit-mask spectroscopy with Daniel Stern, Adam Stanford and Alison Coil. Some of the data presented herein were obtained at the W. M. Keck Observatory, which is operated as a scientific partnership among the California Institute of Technology, the University of California and the National Aeronautics and Space Administration. The Observatory was made possible by the generous financial support of the W. M. Keck Foundation. This paper is based on observations made with the NASA/ESA *Hubble Space Telescope*, obtained from the Data Archive at the Space Telescope Science Institute, which is operated by the Association of Universities for Research in Astronomy, Inc., under NASA contract NAS 5-26555. We are grateful to the GOODS team for making their reduced images public. ERS acknowledges a Particle Physics and Astronomy Research Council (PPARC) studentship supporting this study.

## REFERENCES

- Binette L., Wang J. C. L., Zuo L., Magris C. G., 1993, *AJ*, 105, 797  
 Bunker A. J., Moustakas L. A., Davis M., 2000, *ApJ*, 531, 95  
 Charlot S., Fall S. M., 1993, *ApJ*, 415, 580  
 Davis M. et al., 2002, *SPIE*, in press (astro-ph/0209419)  
 Dey A., Spinrad H., Stern D., Graham J. R., Chaffee F. H., 1998, *ApJ*, 498, L93  
 Dickinson M., Giavalisco M., 2002, in Bender R., Renzini A., eds, *ESO Astrophysics Symposia Series, The Mass of Galaxies at Low and High Redshift*. Springer-Verlag, Berlin, p. 324  
 Ellis R., Santos M. R., Kneib J.-P., Kuijken K., 2001, *ApJ*, 560, L119  
 Fan X. et al., 2001, *AJ*, 122, 2833  
 Ford H. C. et al., 2002, *BAAS*, 200.2401  
 Giacconi R. et al., 2002, *ApJS*, 139, 369  
 Hu E. M., McMahon R. G., Cowie L. L., 1999, *ApJ*, 522, L9  
 Hu E. M., Cowie L. L., McMahon R. G., Capak P., Iwamuro F., Kneib J.-P., Maihara T., Motohara K., 2002, *ApJ*, 568, L75  
 Kodaira K. et al., 2003, *PASJ*, 55, L17  
 Kogut A. et al., 2003, *ApJ*, in press (astro-ph/0302213)  
 Lehnert M. D., Bremer M., 2003, preprint (astro-ph/0212431)  
 Lowenthal J. D. et al., 1997, *ApJ*, 481, 673  
 Madau P., 1995, *ApJ*, 441, 18  
 Malhotra S., Wang J. X., Rhoads J. E., Heckman T. M., Norman C., 2003, *ApJ*, 585, L25  
 Massey P., Gronwall C., 1990, *ApJ*, 358, 344  
 Massey P., Strobel K., Barnes J. V., Anderson E., 1988, *ApJ*, 328, 315  
 Meurer G. R., Heckman T. M., Lehnert M. D., Leitherer C., Lowenthal J., 1997, *AJ*, 114, 54  
 Oke J. B., Korycansky D. G., 1982, *ApJ*, 255, 11

- Osterbrock D. E., 1989, *Astrophysics of Gaseous Nebulae and Active Galactic Nuclei*. University Science Books, Mill Valley, CA
- Pettini M., Shapley A., Steidel C. C., Cuby J.-G., Dickinson M., Moorwood A. F. M., Adelberger K. L., Giavalisco M., 2001, *ApJ*, 554, 981
- Phillips A. C., Faber S., Kibrick R., Wallace V. (DEIMOS Team), 2002, *BAAS*, 203, 137.02
- Rhoads J. E. et al., 2003, *AJ*, 125, 1006
- Schneider D. P., Schmidt M., Gunn J. E., 1991, *AJ*, 101, 2004
- Stanway E. R., Bunker A. J., McMahon R. G., 2003, *MNRAS*, 342, 439
- Steidel C. C., Pettini M., Hamilton D., 1995, *AJ*, 110, 2519
- Steidel C. C., Giavalisco M., Pettini M., Dickinson M. E., Adelberger K. L., 1996, *ApJ*, 462, L17
- Steidel C. C., Adelberger K. L., Giavalisco M., Dickinson M. E., Pettini M., 1999, *ApJ*, 519, 1
- Steidel C. C., Adelberger K. L., Shapley A., Pettini M., Dickinson M. E., Giavalisco M., 2000, *ApJ*, 532, 170
- Stern D., Bunker A., Spinrad H., Dey A., 2000, *ApJ*, 537, 73
- Warren S. J., Møller P., 1996, *A&A*, 311, 25

This paper has been typeset from a  $\text{\TeX}/\text{\LaTeX}$  file prepared by the author.

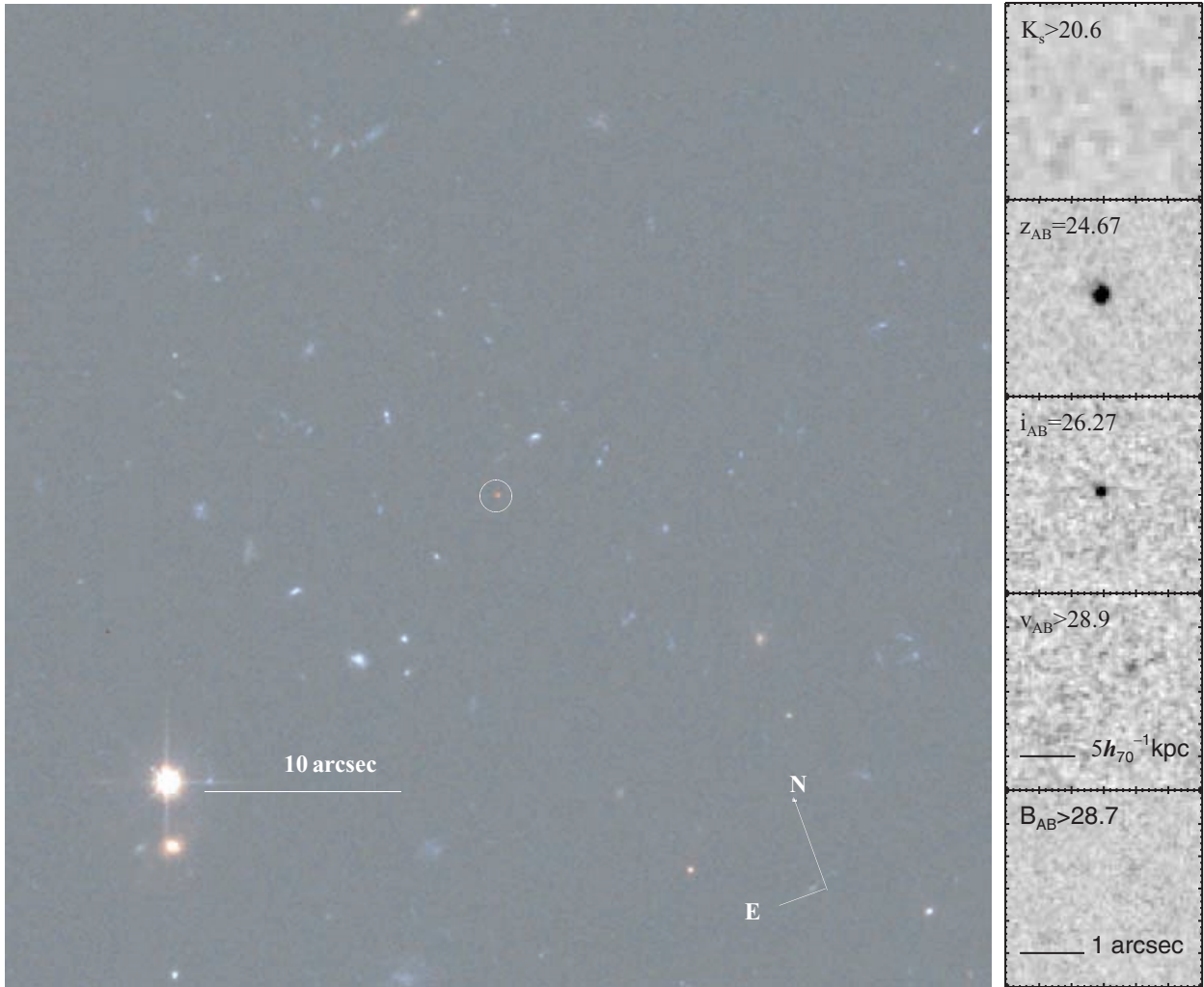


**Figure 3.** Three-colour picture from *HST/ACS* GOODS imaging of the CDF-S, formed from the first three epochs of observation. The red channel is the F850LP  $z'$  band (6 ks), green is the F775W  $i'$  band (3 ks), and blue is the F606W  $v$  band (3 ks). The  $z = 5.78$  galaxy SBM03#3 is at the centre, and is the reddest object in the field (the only  $i'$ -drop). The field of view is  $50 \times 50 \text{ arcsec}^2$ . The  $B$ ,  $v$ ,  $i'$ ,  $z'$  and  $K_s$  images are shown on the right (3 arcsec across).